Regional subsidence analysis in the Vienna Basin (Austria)

Monika HÖLZEL[1)*)], Michael WAGREICH[1)], Robert FABER[2)] & Philipp STRAUSS[3)]

[1)] Department of Geodynamics and Sedimentology, University of Vienna, Centre for Earth Sciences, Althanstr. 14, 1090 Vienna, Austria

[2)] Terramath, Hauptstr. 59, 3021 Pressbaum, Austria

[3)] OMV Exploration & Production GmbH, Gerasdorferstr. 151, 1210 Vienna, Austria

[*)] Corresponding author, monika.hoelzel@univie.ac.at

Abstract

In the southern and central parts of the Vienna Basin in Austria, 50 wells have been investigated to quantify the subsidence during the pull-apart stage of basin evolution (Middle to Upper Miocene; 16.1 – 7.8 Ma). Subsidence analysis is based on the decompaction of the sedimentary record at the time of interest, with the results displayed as total basement and tectonic subsidence curves and tectonic subsidence rates for a given time interval. Due to the compartmentalisation of the basin floor and the overlying sediments, the results vary in detail. They show the highest tectonic subsidence rates occurred during the Upper Lagenid Zone (14.5 – 14.2 Ma) with c. 1000 m/Ma in the southern part and around 700 m/Ma in the central part of the basin. Three types of subsidence curve have been distinguished, representing combinations of three main subsidence phases; in the early Badenian, the Sarmatian, and the Middle Pannonian. Maps of the cumulative tectonic subsidence of four selected stratigraphic tops and the interval tectonic subsidence of four stratigraphic zones are presented.

Im südlichen und zentralen Teil des Wiener Beckens (Österreich) wurden zur Quantifizierung der Subsidenz 50 Bohrungen untersucht. Als Zeitraum wurde die Entwicklung der Pull-Apart Phase (Mittleres bis Oberes Miozän, 16.1 – 7.8 Ma) gewählt. Die Subsidenzanalyse basiert auf der Dekompaktion der Sedimente zu bestimmten Zeitpunkten. Die Ergebnisse sind als Gesamt-Basement- und tektonische Subsidenz und Kurven tektonischer Subsidenzraten für bestimmte Zeitintervalle dargestellt. Im Detail variieren die Kurven, weil der Beckenuntergrund und die darüberliegenden Sedimente in Blöcke zerteilt sind. Die höchsten Werte der tektonischen Subsidenzraten ergeben sich in der Oberen Lageniden Zone (14,5 – 14,2 Ma) mit ca. 1000 m/Ma im südlichen Teil und mit niedrigeren Werten um die 700 m/Ma im zentralen Teil. Beim Vergleich der Form dieser Kurven ergaben sich 3 Hauptsubsidenzphasen für das frühe Badenium, für das Sarmatium und im Mittelpannonium. Als Endergebnisse präsentieren wir Karten der kumulativen tektonischen Subsidenz von 4 ausgewählten stratigraphischen Grenzen und der Intervall-Subsidenz von 4 stratigraphischen Zeitabschnitten.

1. Introduction

A large number of publications about the formation and geological evolution of the Vienna Basin has been published, beginning with classic papers in the 19th century (e.g. Keferstein, 1828) up to recent articles on sequence stratigraphy and tectonics. Here, we present a detailed quantification of subsidence in the Vienna Basin through time. Subsidence analysis allows a quantitative reconstruction of basin evolution, sediment influx and deposition, and gives hints to the timing and types of tectonic driving forces. Due to the extensional basin formation, a complex fault pattern evolved in the Vienna Basin, with duplexes along sinistral strike-slip systems and normal faulting during the Middle to Upper Miocene. This resulted in the obvious tectonic segmentation of the basin fill, which, consequently, calls for detailed subsidence analysis, using a larger data base than previously used (e.g. Lankreijer at al, 1995).

The data presented here were derived from 50 wells drilled in the southern and central Vienna Basin (Austrian part, Fig. 1) and, due to the high density of boreholes, allows the plotting of detailed regional subsidence maps. Other publications on this topic have mainly referred to surrounding areas, such as the eastern part of the foreland-basin of the Eastern Alps

(Genser et al., 2007), the Styrian Basin (Sachsenhofer et al., 1997) and the Pannonian Basin System (Sclater et al., 1980; Lankreijer at al, 1995; Lankreijer, 1998, Baldi et al., 2001). Lankreijer (1998) quantified the large-scale subsidence of the whole Pannonian system, including the Vienna Basin. Lankreijer et al. (1995) integrated 36 wells from the Slovakian northern part and 12 wells from the Austrian central part of the Vienna Basin. Our work, which mainly covers the remaining parts of the Vienna Basin, aims to give a more detailed regional study and interpretation of subsidence patterns, using a significantly revised, more accurate stratigraphy of the Vienna Basin, developed since the 1990s (Rögl, 1996; Steininger and Wessely, 1999; Rögl et al., 2002; Harzhauser et al., 2002; Harzhauser and Piller, 2004; Piller et al., 2004; Strauss et al., 2006; Hohenegger et al., 2008). Together with the high density of borehole data, this has allowed considerable refinements to be made in the timing of subsidence events and more accurate tectonic interpretations.

2. Geological Outline of the Vienna Basin

The main subsidence period of the Vienna Basin was during the Miocene. The initial basin structure was a wedge-top

zone (DeCelles and Giles, 1996) on the frontal parts of the north-west propagating thrust sheets of the Eastern Alps (Lower Miocene; ~18 – 16 Ma; Fig. 2). Within this zone, mainly fluviatile sediments filled several small basins that later merged into one large basin. Due to changes in the local stress-regime, a pull-apart geometry began to develop (Fodor, 1995; Decker and Peresson, 1996), with the initiation of large-scale sinistral strike-slip fault systems; these are often rooted in reactivated basement structures and were accompanied by significant normal faults with offsets reaching some 1000s of metres. This led to an intense segmentation of the basin into duplexes, where depocentres were filled with clastic sediments up to 5.5 km thick (Middle to Upper Miocene; ~16 – 7 Ma; Fig. 2). Detailed descriptions of the basin evolution can be found in Jiricek and Tomek (1981), Royden (1985), Wessely (1988), Seifert, (1992), Wessely (1992), Fodor (1995), Weissenbäck (1996), Kovác et al. (2004) and Hinsch et al. (2005).

## 3. Principles of Subsidence Calculations

Subsidence analysis is mainly based on decompaction of the sedimentary record (Steckler and Watts, 1978; Van Hinte, 1978; Sclater and Christie, 1980). This uses empirically derived curves of porosity-depth relationships, with an exponential reduction of porosity at increasing depths (Baldwin and Butler, 1985). The most important parameters are the thickness of the sedimentary layers and the chronostratigraphy, both of which affect quantification of the subsidence rates. The total subsidence is partitioned into subsidence caused by the tectonic driving force(s) and subsidence due to the sediment load (and compaction). Backstripping removes the effect of sediment loading and compaction from the basement subsidence. Normally, an Airy isostasy model is applied, with the sediment load replaced by a column of water. The results can be used to infer types of the tectonic driving forces and for basin modelling (Lankreijer et al., 1995; Sachsenhofer et al., 1997). The difference between basement and tectonic subsidence curves are shown in Fig. 3. For further descriptions of the method refer to Einsele (2000) and Allen and Allen (2005).

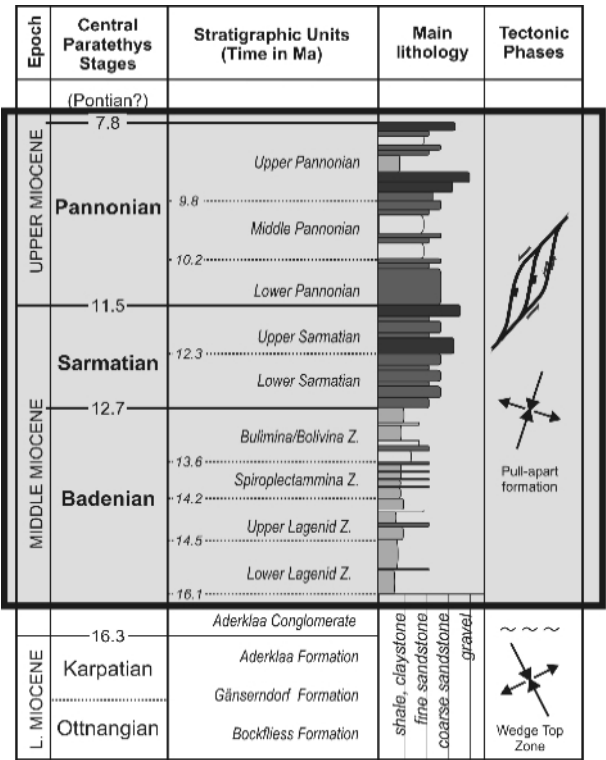For calculating subsidence, the programme DeCompactionTool (DCT) has been developed (Fig. 4; Wagreich, 1991; Hölzel et al., 2008b). This software implements an error quantification on the subsidence analysis, based on Monte Carlo Simulation, such that a range of possible values is assigned to each parameters used. A random function chooses input parameter values within the defined ranges and these are used to calculate the subsidence. From a number of input parameter value combinations, the average subsidence is determined. The programme also incorporates for the first time, the parameter "age", as the controlling factor for the x-axis. Inputting the correct sedimentary age of backstripped layers is particularly crucial for subsidence rate calculations and thus for identifying discrete phases of subsidence. The approach used reduced errors due to ongoing uncertainties in the Vienna Basin chronostratigraphy (Hohenegger et al., 2008).

3.1. Data Base

Input data of wells from the southern and central parts of
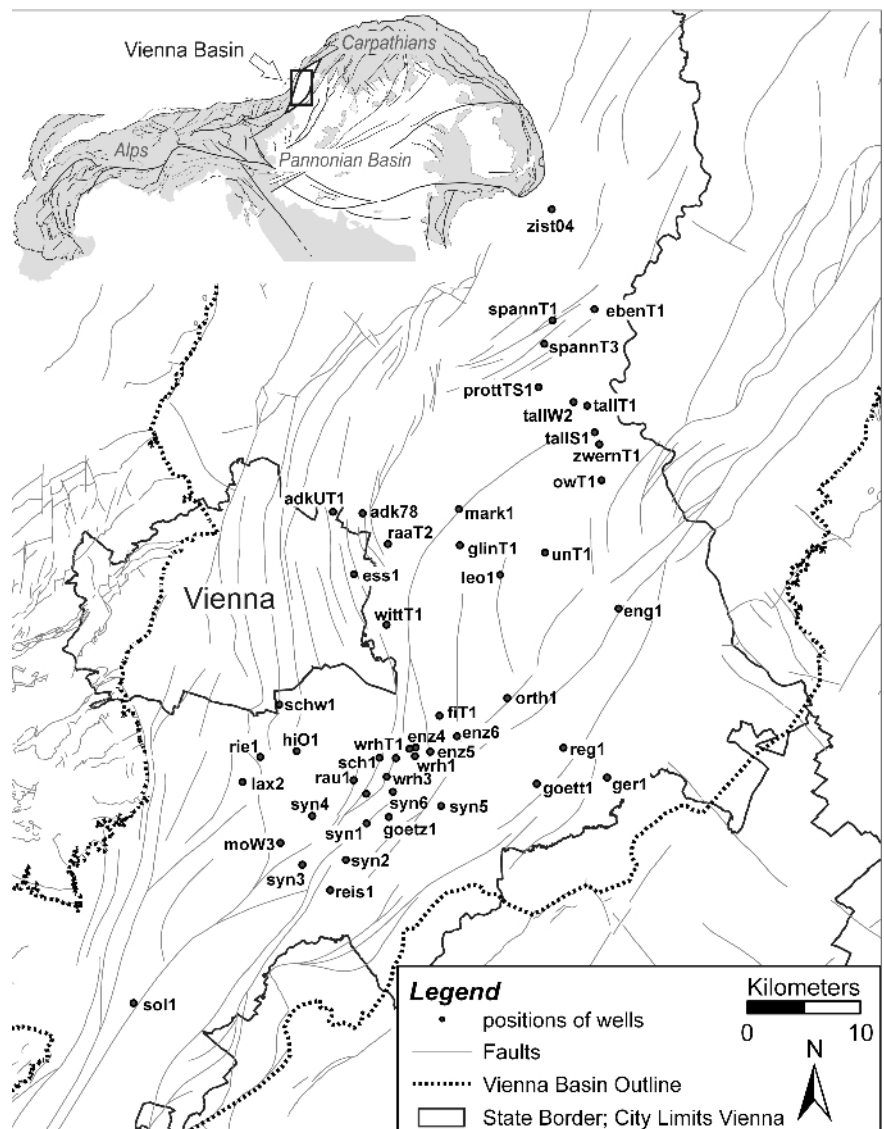
Figure 1: Position of the Vienna Basin within the Alpine/Carpathian transition and overview of borehole locations used in this study.

Epoch	Central Paratethys Stages	Stratigraphic Units (Time in Ma)	Main lithology	Tectonic Phases
		(Pontian?)		
UPPER MIOCENE	Pannonian	7.8 — Upper Pannonian		
		9.8 ···· Middle Pannonian		
		10.2 ···· Lower Pannonian		
		11.5 — Upper Sarmatian		
MIDDLE MIOCENE	Sarmatian	12.3 ···· Lower Sarmatian		
		12.7 —		
	Badenian	Bulimina/Bolivina Z.		Pull-apart formation
		13.6 ···· Spiroplectammina Z.		
		14.2 ···· Upper Lagenid Z.		
		14.5 ···· Lower Lagenid Z.		
		16.1 ····		
L. MIOCENE		16.3 — Aderklaa Conglomerate	shale, claystone / fine sandstone / coarse sandstone / gravel	~ ~ ~
	Karpatian	Aderklaa Formation		
		Gänserndorf Formation		
	Ottnangian	Bockfliess Formation		Wedge Top Zone

Figure 2: Simplified stratigraphic table with Central Paratethys stages and local stratigraphic nomenclature used in the Vienna Basin. The grey rectangle marks the investigated time window. Tectonic phases according to Decker and Peresson (1996).

the Vienna Basin in Austria was provided by OMV-E&P Austria, (Fig. 1). The subsidence curves were calculated for the pull-apart evolution of the basin from 16 to 7 Ma, to quantify the main phase of basin evolution within a constant stress field. The basal level used in the calculations was the top of the Aderklaa Conglomerate, which has been dated to 16.1 Ma (Fig. 2; Weissenbäck, 1996).

The Lower Miocene wedge-top phase of basin development was excluded from the subsidence calculations as it was controlled by a different stress field and different mechanisms of basin formation. Detailed data for that time-period are not available. Furthermore, the angular unconformity between the Kar-
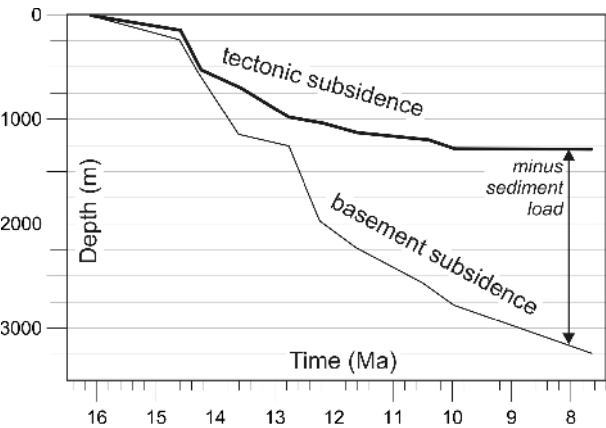
Figure 3: Difference between backstripped tectonic and basement subsidence. Curve is from well raaT2.

patian and Badenian also indicates a major break in basin evolution (Hölzel et al., 2008a). Quaternary strata were also excluded, both because of the recent change to a regional uplifting regime (Decker and Peresson, 1996) and because the stratigraphic record is incomplete.

The following parameters were used: 1.) thickness of stratigraphic layers (metres); 2.) age of stratigraphic boundaries (Ma); 3.) lithology, with percentages attributed to different lithologies; 4.) sedimentation (palaeowater) depth (metres); 5.) decompaction parameters (porosity for t_0 = initial % porosity, decompaction coefficient c, final % porosity) and 6.) physical properties (grain density, crustal density).

Values for some of these parameters were derived from borehole data and related log measurements: Depths to formation tops are necessary to measure the sediment thickness. Most wells reached the basement below the Neogene basin-fill, so that the stratigraphic record for the Middle to Upper Miocene is complete. Chosen wells mostly lie in undisturbed fault blocks, some distance away from the basin margin. Consequently, the thickness of the sedimentary infill was not significantly influenced by faulting or erosion. Missing stratigraphic data and well-data in areas of interest have been interpolated from mapping of stratigraphic boundaries within seismic data. These sections have been termed synthetic wells (*syn*).

The chronostratigraphic time-scale for the Neogene of Austria has been used (Piller et al., 2004) together with the eco-bio-zonation terms for the Vienna Basin (Rögl, 1998; Strauss et al. 2006; M. Harzhauser, pers.comm.).

Well-log data contains information on the lithological composition of the sediments. For this, Self Potential logs (SP logs), in combination with resistivity logs, were mainly used to differentiation between sand and shale. These data were cross-checked with OMV in-house reports about the composition of well-cuttings. The lithology parameter does not show much variation, because in the investigated, largely basinal offshore area, most sediments are composed of sand (-stone), clay and/or siltstone. Carbonate rocks are of minor importance.

Palaeobathymetric data (sedimentation depth) were taken from the compilation of Wagreich and Schmid (2002), which was based on sedimentological and palaeontological investigations (Kreutzer, 1993; Seifert, 1996). Relative sea-level changes have not been incorporated in the calculations, since the basin was separated from the world ocean after 10.5 Ma (Steininger and Wessely, 1999).

Decompaction parameters were compiled from Steckler and Watts (1978), Royden and Keen (1980), Sclater and Christie (1980) Sawyer (1983) and, Bond and Kominz (1984). For the present-day porosity, a value of 10 % has been generally assumed (Flügel and Walitzi, 1968).

3.3. Generation of Subsidence Maps

For an area-wide visualisation of the tectonic subsidence, maps were compiled for distinct stratigraphic boundaries (Fig. 8) and stratigraphic zones (Fig. 9). For the gridding process, the software Surfer© was used. In Austrian Bundesmeldenetz

Coordinates, the defined area ranges from 742,000/302,000 (lower left; UTM M33: 591,650/5 301,089) to 792,000/378,000 (upper right; UTM M33: 640,310/5 377,928). Using the Kriging algorithm, a grid with 200 rows x 100 columns, resulting in an x-spacing of c. 500 m and y-spacing of c. 380 m was generated. Due to the Kriging algorithms and the irregular distribution of data points (boreholes), some isolated spots may occur; however, we used these maps to decipher general trends in the regional distribution of subsidence. Uncertainties due to the extrapolation of isolines to the basin margin were taken into account critically during interpretation and conclusions were drawn only from the central areas of the maps.

4. Results and Interpretation

Only the Middle to Upper Miocene basin subsidence history has been studied in detail because Lower Miocene basin structures were triggered by different basin-forming mechanisms, such as fault propagation folds that were active in the underlying Alpine units (Hölzel et al., 2008a), and thus represent the fill of one or more separate basins.

Results for the Middle to Upper Miocene basin history are presented grouped (for the position of groups see Fig. 5) as basement subsidence in total (BS-Total), tectonic subsidence in total (TS-Total) and as tectonic subsidence rates (TS-Rate; Figs. 6 and Fig. 7).

Many curves show the highest subsidence rates in the Upper Lagenid Zone, the duration of which has become shorter since the 1990s, due to ongoing refinements of the Central Paratethys chronostratigraphy and the local Vienna Basin-zones. Although we are aware that the time factor is one of the most influential parameters in basin analysis, the steepness of the curves in this time interval is not thought to be only an effect of its shorter length, because there are many other curves show different subsidence rates (see below). Consequently, we conclude that these results from the Upper Lagenid Zone are not an artefact of an erroneously defined duration, but represent a robust result.

4.1. Regional Trends of Subsidence

To obtain an accurate impression of the regional differences in the subsidence history, the wells have been sorted into several groups (G1 – G13) based partly on their position, from south to north. Their position within the same fault block bordered by major faults or the occurrence in depocentres which reached the same depth was also used in defining the groups. All well-groups, fault names and key structural features are indicated in Fig. 5.

4.1.1 Groups G1 and G2

The southernmost well is *sol1*. Due to of its isolated position, it has been put into a separate group (G1). The three G2 wells lie in the footwall of the Leopoldsdorf Fault. The BS-Total curve for *lax2*, *rie1* and *schwe1* display a continuous decrease through time. Well *moW3* indicates a stepwise subsidence, which, surprisingly, resembles the curve from well
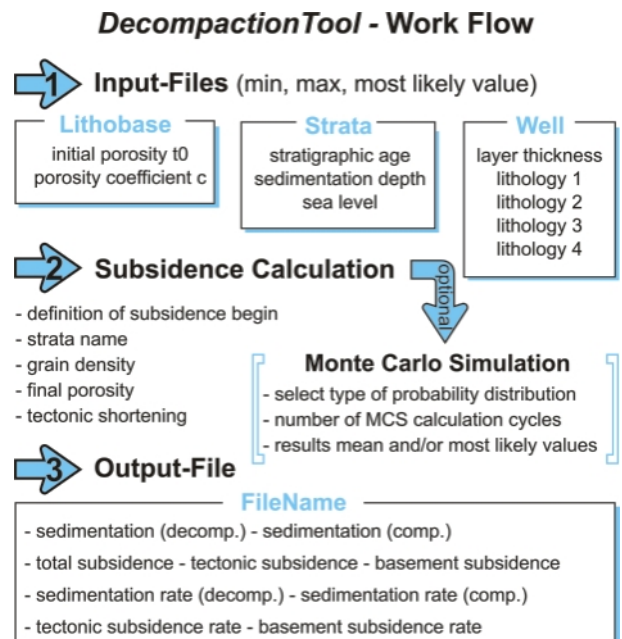
Figure 4: Work flow and input parameters for the software DeCompactionTool (Hölzel et al., 2008b).

sol1. For the TS-Rate each curve is different as *schwe1* and *moW3* show peaks for the Upper Lagenid Zone, Sarmatian and Middle Pannonian. Values from 250 m/Ma – 1000 m/Ma dominate during those phases, in contrast to nearly no subsidence during the remaining time intervals. Wells *lax2* and *rie1* also show the same peaks only in the Upper Lagenid Zone
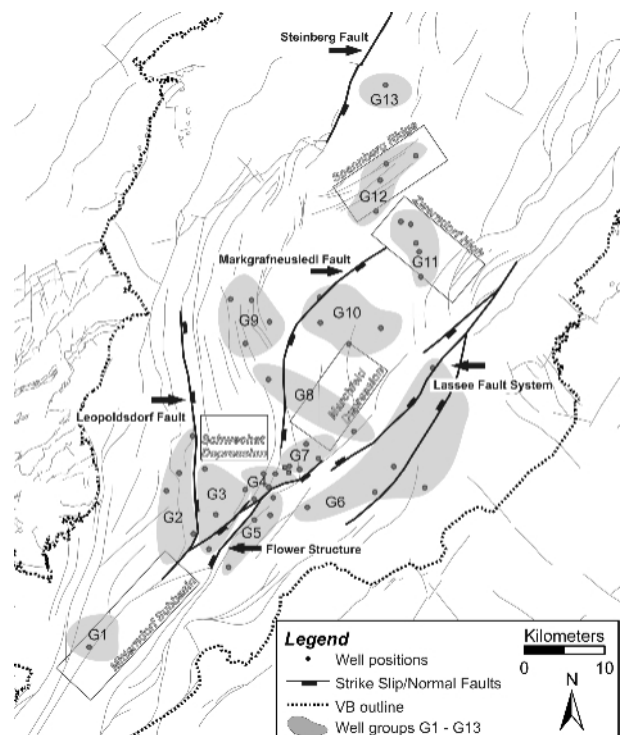
Figure 5: Division of wells into groups according to fault blocks including key structural features of the Vienna Basin such as faults and highs and lows of the top of the pre-Neogene basement (for general position of Vienna Basin and names of wells see Fig. 1).

and Middle Pannonian, but less total subsidence.

4.1.2 GROUP G3

This group (4 wells) comprises data from the hanging wall block of the Leopoldsdorf Fault. The common trend of the BS-Total is high subsidence within the Upper Lagenid Zone, which also correlates with well *moW3* from G2. This may be attributed to surface growth of the Leopoldsdorf Fault, starting with the highest normal displacement in a more northern position. In the Lower Lagenid Zone, the wells *syn4*, *him1*, *rau1* and *syn3* start with moderate TS-Rates of 250 m/Ma, which, in the

Upper Lagenid Zone, increases to 500 m/Ma – 1000 m/Ma. For the rest of the Miocene they subside in a very similar way, with values around 100 – 250 m/Ma. With this pattern of homogeneous subsidence in the hanging wall of the Leopoldsdorf Fault, slip variations along the Leopoldsdorf Fault (Hölzel and Wagreich, 2006) were probably mainly dependent on the behaviour of the footwall block.

4.1.3 GROUP G4

These wells are situated in an area where the normal faults of the negative flower structure of the Mitterndorf sub-basin (Hinsch et al., 2005) displace and rotate blocks vertically. As a result, the wells all show essentially the same subsidence history, although they are separated by faults. The subsidence rates are very similar to those of G2, although it accelerated in the Lower Lagenid Zone, with a moderate TS-Rate of c. 250 m/Ma for the rest of the basin evolution.

4.1.4 GROUP G5

The wells *syn2* and *rei1* are situated in the highest parts of the eastern footwall of the negative flower structure. This area forms a relay ramp to the north and all other wells of this group lie in a deeper position along the ramp. As a consequence, BS-Total of *syn2* and *rei1* do not display an increase of subsidence in the Upper Lagenid Zone comparable to that seen in the other wells, *syn1*, *goetz1* and *syn6*. Sarmatian and Middle Pannonian phases are rather subdued or not represented in TS-Rates, indicating that this part of the basin was not affected by significant extension during later stages of basin evolution.

4.1.5 GROUP G6

The BS-Total curves of *ger1* and *goett1* show the same development at the beginning of the Upper Lagenid Zone, with parallel segments. The curves then differ because of the higher position of well *ger1* in the footwall of the Lassee Fault, which, therefore, could have been active, with a normal offset, from the Upper Lagenid Zone onwards. Wells *reg1* and *syn5* are
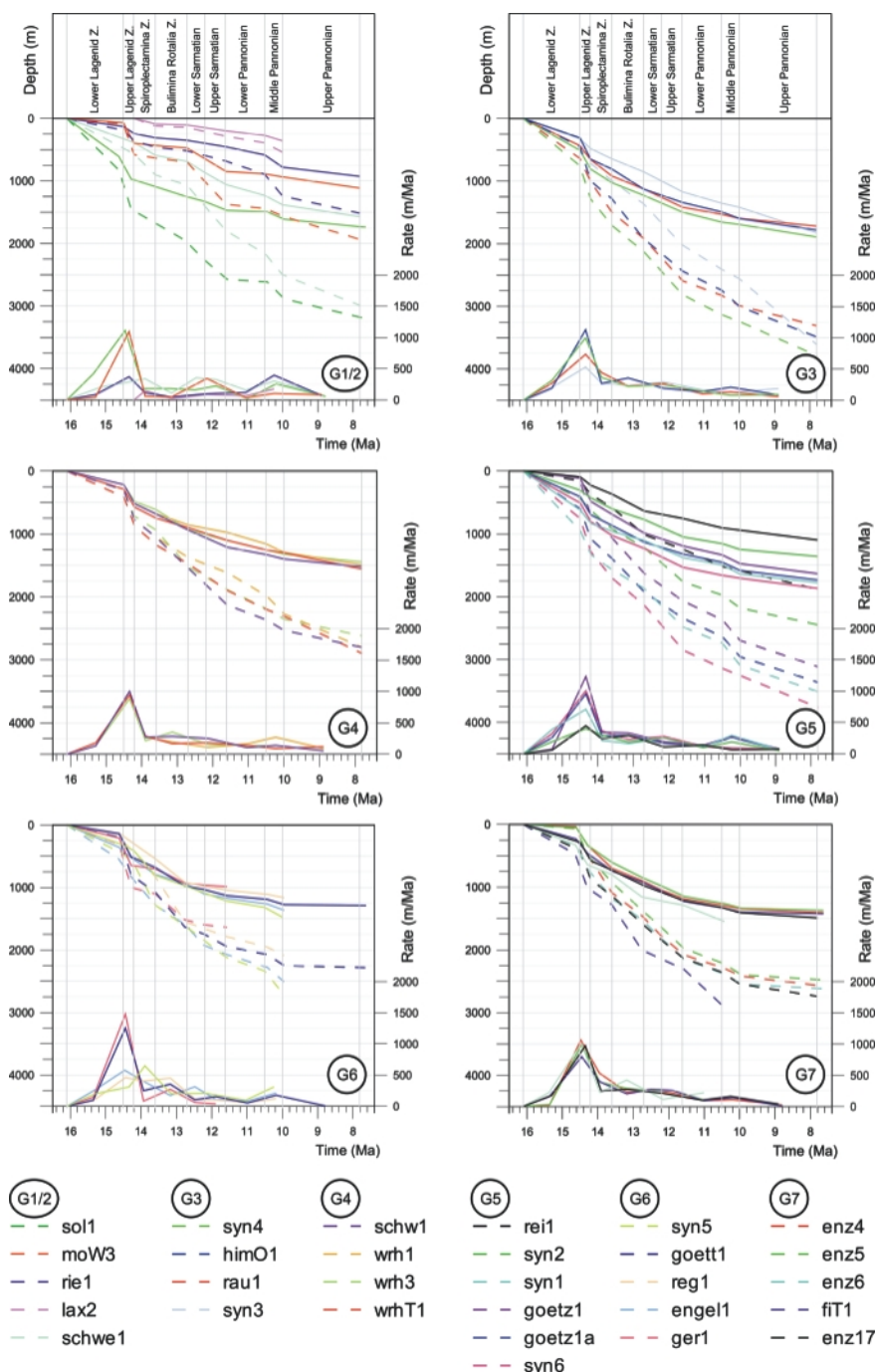
FIGURE 6: Groups 1-7: Basement subsidence total (BS-Total, dashed lines), tectonic subsidence total (TS-Total, solid lines) and tectonic subsidence rates (TS-Rates, solid lines).

similar, because they lie in the same fault block. TS-Rates display the same pattern as G5, with no, or only very minor Sarmatian and Pannonian phases.

4.1.6 Group G7

Wells of this group are situated in a strongly faulted area, in which fault blocks are bordered by various narrow branches of the negative flower structure. The BS-Total results seem to resemble steady subsidence except during the Lower Lagenid Zone; the TS-Rates are similar to G5 and G6, with only one significant subsidence phase, in the Badenian.

4.1.7 Group G8

Well *witt1* is situated at the northern flank of the Schwechat Depression and *orth01* lies within the Marchfeld Depression; both depressions display high basement subsidence values for the Vienna Basin, of up to 4000 m. Both wells have parallel BS-Total curves in the Badenian, but antithetic curves for the other time intervals. This has been interpreted as the result of switching depocentres and sediment input; if one depocenter was active, the other one was inactive and vice versa. BS-Total for well *fiT1* of G7 is similar to well *orth1*, except during the Pannonian, because the sediment record ends at the top Lower Pannonian. TS-Rates indicate 3 phases of subsidence, with Badenian subsidence being the highest (up to 1500m/Ma) and Middle Pannonian subsidence being the lowest (below 250m/Ma).

4.1.8 Group G9

The BS-Total trends of wells *ess1*, *raaT1* and *adk78* and *adkUT1* are very similar, typical for the area between the Markgrafneusiedl Fault and the Leopoldsdorf Fault, in the central part of the Vienna Basin, southwest of the Spannberg Ridge. TS-Rates again display a threefold pattern, similar to G8, but with lower rates in the Badenian.

4.1.9 Group G10

This group largely resembles G9 for the BS-Total values. The trends of *mark1*, *glinz1* and *unT1* are the same. Well *leo1*, which shows a

unique trend in having a broadly distributed Late Badenian subsidence that has been attributed to fault interference west of the Markgrafneusiedl Fault. The TS-Rates do not exceed 450 m/Ma, but the development from the Upper Sarmatian onwards coincides with the other wells of G9 and G10. Well *leo1* again shows a considerable difference to all other wells in the central part of the basin.

The areas covered by G8 – G10 subsided together in a largely similar way. This indicates that the Markgrafneusiedl Fault is a very young feature, with post sedimentary activity from the Upper Pannonian onwards.
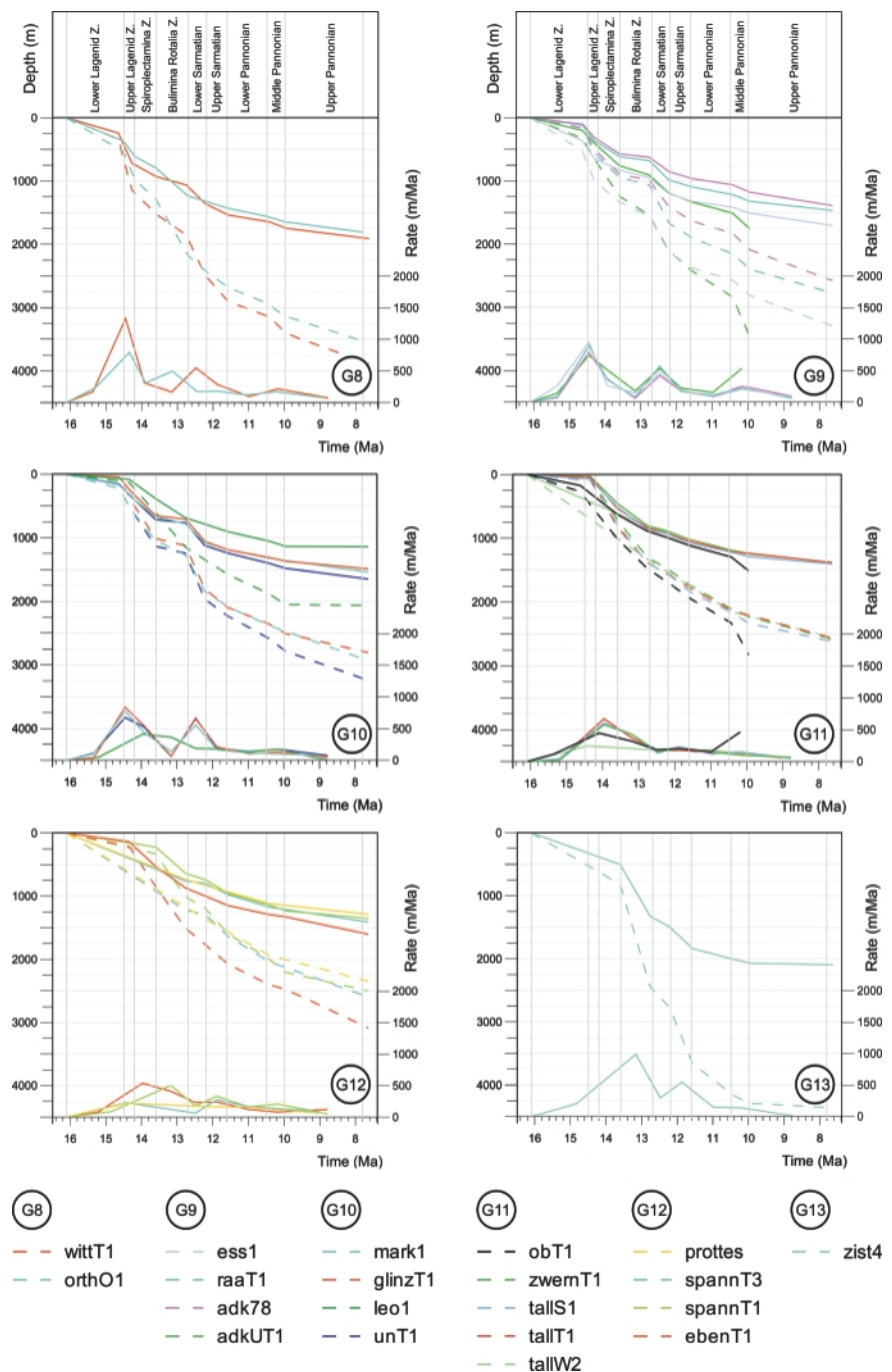

Figure 7: Groups 8-13: Basement subsidence total (BS-Total, dashed lines), tectonic subsidence total (TS-Total, solid lines) and tectonic subsidence rates (TS-Rates, solid lines).

4.1.10 Groups G11 and G12

In the sedimentary columns of G11 and G12, the Lower Lagenid Zone is missing and, consequently, subsidence curves start later. The Badenian transgression was not able to reach this area of the former coast line, at the flanks of the Spannberg Ridge and the Zwerndorf High (e.g. Weissenbäck, 1996). Thus sedimentation started significantly later and a depocenter for the transgressing sediments had not been established. The basement structure of the Spannberg Ridge was uplifted during the Upper Karpatian (Hölzel et al., 2008a). Consequently, TS-Rates display a delay in subsidence in relation to data

phases resemble curves from G10.

4.2. Subsidence Maps

Figures 8 and 9 show total tectonic subsidence for the central and southern part of the Vienna Basin, plotted as relative depth maps for distinct tops of stratigraphic units and interval subsidence between these stratigraphic boundaries, respectively. The time intervals range from 1.1 – 1.7 Ma, except for the Upper Lagenid Zone, which is considerably shorter, most probably representing only 300,000 years (Fig. 2).

The top Lower Lagenid Zone subsidence pattern shows the characteristic segmentation into narrow depocentres (Fig. 8a) due to the formation of strike-slip duplexes. In the southern part, the hanging wall of the Leopoldsdorf Fault subsided considerably in relation to the footwall, indicating the synsedimentary movement of this fault during the Lower Lagenid Zone. In the central part, uplifted basement blocks, such as the Spannberg Ridge, are displayed by zero values. The strong subsidence segmentation suggests major fault activity during the Lower Lagenid Zone. The interval subsidence maps show that in the following depocentres merged (Fig. 9a). During the early Badenian (Fig. 9b), the Zwerndorf High developed, with only 200 m total tectonic subsidence, in contrast to the more southern regions, which subsided by up to 600 m during the same time-interval. At the Badenian/Sarmatian boundary, the delay in subsidence from the central to the northern part is visible (Fig. 8c). From the late Badenian to the top Sarmatian (Fig. 9c), this trend reversed, with pronounced subsidence in the Zwerndorf area (600 m) and lower subsidence values within the Marchfeld Depression
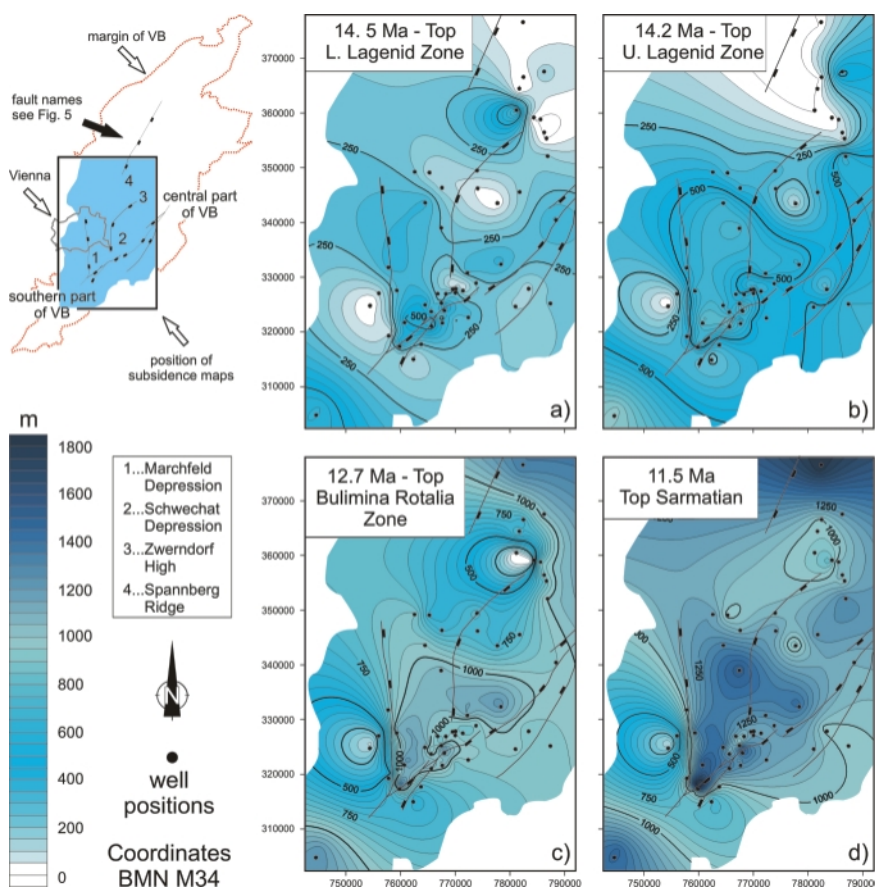
Figure 8: Tectonic subsidence maps of the central and southern Vienna Basin displayed as cumulative subsidence at 4 stratigraphic boundaries. Extrapolated isolines to the basin margin must not be interpreted, because they represent artificial borders.

from surrounding, lower-lying areas with respect to the Spannberg Ridge, like well *ebenT1*.

4.1.11 Group G13

Well *zist4* was drilled into the hanging wall of the Steinberg Fault. For the lower parts of the well, the TS-Rate shows maxima within the Spiroplectamina Zone (1000 m/Ma) and in the Sarmatian (250 – 500 m/Ma). These values contradict former assumptions that the strongest activity on this major basin forming fault was during the Lower Badenian, but it coincides with the varying thicknesses of growth strata through time observed on seismic sections. The two pronounced subsidence

(only up to 400 m). In the southern part of the basin, the fault blocks of the negative flower structure subsided c. 600 m. The top Sarmatian (Fig. 8d) indicates that the overall tectonic subsidence was higher in the southern part (1500 m) than in the central part (1000 m). The Sarmatian to Middle Pannonian pattern (Fig. 9d) shows ongoing uniform subsidence with moderate values affecting the deeper parts of the Vienna Basin, whereas the marginal areas remain nearly stable.

4.3. General Subsidence Trends

In general, the subsidence curves of the Vienna Basin display a typical pattern for strike-slip basins, with very high sub-

sidence rates (up to > 1000 m/Ma), but in only short phases, and a general "concave-up" shape (Allen and Allen, 2005).

The calculated TS rates are significant for interpreting the subsidence patterns and the tectonic driving forces of basin formation. To discriminate phases of increased subsidence, the TS-Rate curves were divided into 3 types based on their shapes (Fig. 10). There is one (*type A*) with high rates in the Badenian decaying continuously through the rest of the Miocene. The second type (*type B*) includes the Badenian signal but has an additional subsidence peak within the Sarmatian. *Type C* has 3 peaks, with the Badenian and Sarmatian peaks followed by a weaker signal in the Middle Pannonian.

Type A, with a major early Badenian subsidence event followed by decreasing subsidence, has been documented in previous investigations and conforms to the general pull-apart stretching model assumed for the Vienna Basin (Sclater et al., 1980; Lankreijer et al., 1995 and Baldi et al., 2001). Based on 2 boreholes, Baldi et al. (2001) calculated about 500 m of rapid subsidence in the Pannonian Basin during this time interval. In the early Badenian, uniform subsidence started and affected nearly the whole Carpatho-Pannonian area (Sclater et al., 1980). However, our results differ from others (e.g. Wagreich and Schmid, 2002) as the Karpatian was not included in the calculations, as different mechanisms for the Lower Miocene basin formation have been inferred. Large areas, which today lie outside the Vienna Basin, lay within the former Lower Miocene wedgetop zone. Subsidence occurred locally and was mainly governed by the synsedimentary thrusting of the underlying Alpine units. This basin phase essentially ended in the Middle Miocene, with the initiation of the pull-apart Vienna Basin. Therefore, the subsidence values presented here only include (Lower) Badenian data and strongly suggest a solely Badenian "rifting" event of strike-slip basin formation. The Sarmatian signal, which reaches to around half that of the Badenian subsidence rate, is comparable to a minor Sarmatian phase in the Styrian Basin (Sachsenhofer et al., 1997) with an estimated stretching factor of < 1.05. Minor extension is also implied by our data, as Sarmatian tectonic subsidence rates are always lower than Badenian subsidence rate maxima. This Sarmatian phase seems to reflect a common development for the basins at the eastern margin of the Eastern Alps and might be

a product of regional extensional tectonics related to a late phase of lateral extrusion.

The Pannonian subsidence phase shows maximum values of about half that of the Sarmatian subsidence. This can be correlated to the major basin-forming subsidence phase of the nearby Pannonian Basin, because of their co-eval occurrence and the position of the Vienna Basin, at the periphery of the Pannonian Basin System. This significant Pannonian subsidence was not recorded by previous workers, who proposed only subdued subsidence or subsidence termination in the Pannonian (e.g. Sclater et al., 1980; Royden, 1985).
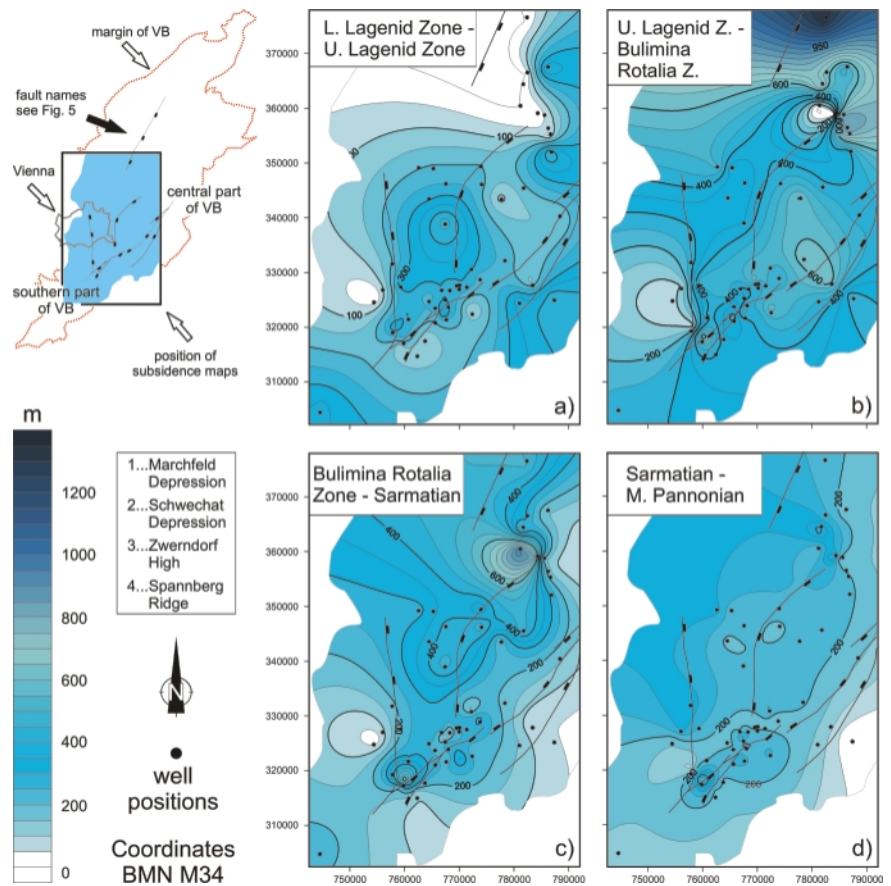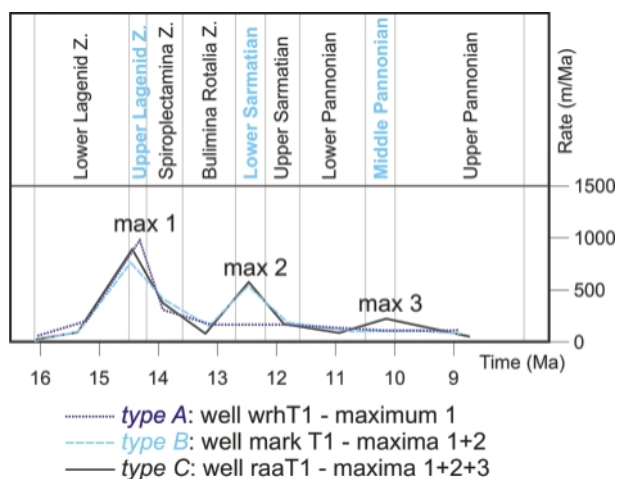

FIGURE 9: Maps of tectonic subsidence of 4 stratigraphic intervals.

Sclater et al. (1980) presumed a uniform stretching of a factor 2 with subsequent lithospheric cooling, which explains their rapid first subsidence phase (Badenian) and the slower linear second phase from the Sarmatian onward, ending during the Pannonian. However, their investigations were based on only one borehole from the centre of the Vienna Basin. Royden (1985) also indicated only one major extensional pull-apart phase, without a significant Pannonian subsidence pulse. Lankreijer et al. (1995) indicated more than one subsidence phase; in the Karpatian-Badenian, in the late Badenian to early Sarmatian and in Pontian to Pliocene times. This threefold subsidence path largely corresponds to our refined results, although the timing differs due recent improvements in the

Figure 10: Three different curve shapes of tectonic subsidence rates as base for the classification of subsidence phases.

basin chronostratigraphy. However, this Pontian to Pliocene subsidence cannot be compared to the Middle Pannonian phase documented here, as Lankreijer et al. (1995) relied strongly on younger, Plio-Pleistocene subsidence, as recorded in the Mitterndorf subbasin, which is clearly separated in time from our Middle Pannonian pulse.

The subsidence modelling of Lankreijer et al. (1995) indicated that the Vienna Basin shows a trend from thin-skinned extension in the north-eastern part to whole lithospheric extension in the central-southern part. Stretching values between 1.04 and 1.30 for the crustal extension and between 1 in the northern part and 1.60 in the southern part for lithospheric extension were proposed. This modelling did not account for separate phases of subsidence, but relied on strong initial Karpatian and Badenian subsidence, followed by minor thermal subsidence. Such a model only accounts for our type A, with curves showing only one subsidence phase, followed by rapidly decaying values.

5. Conclusions

The Vienna Basin is located at the transition between the Eastern Alps, the Carpathians and the Pannonian Basin System. In this special position, the basin underwent more than one phase of subsidence during the Miocene pull-apart tectonism. The general trends imply that the major phase of formation started in the Badenian (Upper Lagenid Zone - Bulimina Rotalia Zone; Middle Miocene). Some of the backstripped wells show a decrease of subsidence throughout the Miocene, but, due to the intense internal segmentation of the basin, other wells display significant subsidence phases in the Sarmatian and Middle Pannonian also. These phases are comparable to events in the Styrian and Pannonian basins. As a result of chronostratigraphic refinements and the high density of boreholes, this study has shown that the interpretation of the overall subsidence pattern is not as simple as previously thought. Regionally or locally, the effects of at least three successive phases of extension, related to the late stage of Alpine-Carpathian orogeny and the ongoing lateral extrusion

and Pannonian Basin formation, have been found in the Vienna Basin. This indicates that these tectonically related areas were influenced by each other during basin evolution and indicate that more than one extensional basin phase occurred during the Middle to Upper Miocene.

References

Allen, P. A. and Allen, J. R. L. (2005). Basin Analysis. Blackwell Scientific Publications, Oxford, 549 pp.

Baldi, K., Benkovics, L. and Sztano, O. (2001). Badenian (Middle Miocene) basin development in SW-Hungary: subsidence history based on quantitative paleobathymetry of foraminifera. International Journal of Earth Sciences, 91, 490-504.

Baldwin, B. and Butler, C. O. (1985). Compaction Curves. AAPG Bulletin, 69, 622-626.

Bond, G. C. and Kominz, M. A. (1984). Construction of tectonic subsidence curves for the early Paleozoic miogeocline, southern Canadian Rocky Mountains: Implications for subsidence mechanisms, age of breakup, and crustal thinning. Geological Society of America Bulletin, 95, 155-173.

DeCelles, P. G. and Giles, K. A. (1996). Foreland basin systems. Basin Research, 8, 105-123.

Decker, K. and Peresson, H. (1996). Tertiary kinematics in the Alpine-Carpathian-Pannonian system: links between thrusting, transform faulting und crustal extension. In: Wessely, G. and Liebl, W. (eds.), Oil and Gas in Alpidic Thrustbelts and Basins of Central and Eastern Europe. EAGE Special Publication, pp. 69-77.

Einsele, G. (2000). Sedimentary Basins - Evolution, Facies, and Sediment Budget. Springer, Berlin, 792 pp.

Flügel, H. W. and Walitzi, E. M. (1968). Regelung und Porosität in Tonmergeln des Wiener Beckens. Neues Jahrbuch für Geologie und Paläontologie, Monatshefte, 1968, 1-11.

Fodor, L. (1995). From transpression to transtension: Oligocene-Miocene structural evolution of the Vienna Basin and the East-Alpine-Western Carpathian junction. Tectonophysics, 242, 151-182.

Genser, J., Cloetingh, S. A. P. L. and Neubauer, F. (2007). Late orogenic rebound and oblique Alpine convergence: New constraints from subsidence analysis of the Austrian Molasse basin. Global and Planetary Change, 58, 214-223.

Harzhauser, M., Daxner-Höck, G. and Piller, W. (2002). An integrated stratigraphy of the Pannonian (Late Miocene) in the Vienna Basin. Austrian Journal of Earth Sciences, 95/96, 6-19.

Harzhauser, M. and Piller, W. E. (2004). The Early Sarmatian - hidden seesaw changes. Courier Forschungs-Institut Senckenberg, 246, 89-111.

Hinsch, R., Decker, K. and Wagreich, M. (2005b). 3-D mapping of segmented active faults in the southern Vienna Basin. Quaternary Science Reviews, 24, 321-336.

Hohenegger, J., Coric, S., Khatun, M., Rögl, F., Rupp, C., Selge, A., Uchman, A. and Wagreich, M. (2008). Cyclostratigraphic dating in the Lower Badenian (Middle Miocene) of the Vienna Basin (Austria): the Baden-Sooss core. International Journal of Earth Sciences, DOI 10.1007/s00531-007-0287-7.

Hölzel, M. and Wagreich, M. (2006). Miocene fault activity in the southern Vienna Basin based on fault backstripping. EGU 2006, Vienna, Geophysical Research Abstracts, 8, EGU06-A-06999.

Hölzel, M., Decker, K., Zámolyi, A., Strauss, P. and Wagreich, M. (2008a). The transition from piggy back to pull-apart in the Vienna Basin (Austria-Slovakia-Czech Republic). EGU Geophysical Research Abstracts, 10, EGU2008-A-04689.

Hölzel, M., Faber, R. and Wagreich, M. (2008b). DeCompaction Tool: Software for subsidence analysis including statistical error quantification. Computers & Geosciences, 34, 1454-14960.

Jiricek, R. and Tomek, C. (1981). Sedimentary and Structural Evolution of the Vienna Basin. Earth Evolution Sciences, 1, 195-206.

Keferstein, C. (1828). Beobachtungen und Ansichten über die geognostischen Verhältnisse der nördlichen Kalkalpenkette in Österreich und Bayern. Deutschland geognostisch-geologisch dargestellt.

Kovác, M., Barath, I., Harzhauser, M., Hlavaty, I. and Hudackova, N. (2004). Miocene depositional systems and sequence stratigraphy of the Vienna Basin. Courier Forschungs-Institut Senckenberg, 246, 187-212.

Kreutzer, N. (1993). Das Neogen des Wiener Beckens. In: Brix, F. and Schultz, O. (eds.), Erdöl und Erdgas in Österreich. Naturhistorisches Museum & F. Berger, pp. 232-248.

Lankreijer, A., Kovac, M., Cloetingh, S., Pitonak, P., Hloska, P. and Biermann, C. (1995). Quantitative subsidence analysis and forward modelling of the Vienna and Danube basins: thin-skinned versus thick-skinned extension. Tectonophysics, 252, 433-451.

Lankreijer, A. C. (1998). Rheology and basement control on extensional basin evolution in Central and Eastern Europe: Variscan and Alpine-Carpathian-Pannonian tectonics. Amsterdam, Vrije Universiteit 158.

Piller, W., Egger, H., Gross, M., Harzhauser, M., Hubmann, B., van Husen, D., Krenmayr, H.-G., Krystyn, L., Lein, R., Mandl, G., Rögl, F., Roetzel, R., Rupp, C., Schnabel, W., Schönlaub, H. P., Summesberger, H. and Wagreich, M. (2004). Die Stratigraphische Tabelle von Österreich 2004 (Sedimentäre Schichtfolgen). Berichte des Instituts für Erdwissenschaften K.-F.-Universität Graz, 329-330.

Rögl, F. (1996). Stratigraphic correlation of the Paratethys (Oligocene and Miocene). Mitteilungen der Geologischen Gesellschaft österreichischer Bergbaustudenten, 41, 65-73.

Rögl, F. (1998). Palaeogeographic considerations for Mediterranean and Parathetys Seaways (Oligocene to Miocene). Annalen des Naturhistorischen Museums in Wien, 99, 279-310.

Rögl, F., Spezzaferri, S. and Coric, S. (2002). Micropaleontology and biostratigraphy of the Karpatian-Badenian transition (Early-Middle Miocene boundary) in Austria (Central Paratethys). Courier Forschungs-Institut Senckenberg, 237, 47-67.

Royden, L. and Keen, C. E. (1980). Rifting process and thermal evolution of the continental margin of eastern Canada determined from subsidence curves. Earth and Planetary Science Letters, 51, 343-361.

Royden, L. (1985). The Vienna Basin: A thin-skinned pull-apart basin. In: Biddle, K.T. and Christie-Blick, N. (eds.). Strike-slip deformation, basin formation, and sedimentation. SEPM Special Publication 37, 320-338.

Sachsenhofer, R. F., Lankreijer, A., Cloetingh, S. and Ebner, F. (1997). Subsidence analysis and quantitative basin modelling in the Styrian Basin (Pannonian Basin System, Austria). Tectonophysics, 272, 175-196.

Sawyer, D. S. (1983). Total tectonic subsidence and the mechanism of rifting at the U.S. Atlantic margin. Eos, Transactions, American Geophysical Union, 64, 851-852.

Sclater, J. G. and Christie, P. A. F. (1980). Continental stretching; an explanation of the post-Mid-Cretaceous subsidence of the central North Sea basin. Journal of Geophysical Research, 85, 3711-3739.

Sclater, J. G., Royden, L., Horvath, F., Burchfiel, B. C., Semken, S. and Stegena, L. (1980). The formation of the intra-Carpathian basins as determined from subsidence data. Earth and Planetary Science Letters, 51, 139-162.

Seifert, P. (1992). Palinspastic reconstruction of the easternmost Alps between Upper Eocene and Miocene. Geologica Carpathica, 43, 327-331.

Seifert, P. (1996). Sedimentary-tectonic development and Austrian hydrocarbon potential of the Vienna Basin. In: Wessely, G. and Liebl, W. (eds.), Oil and Gas in Alpidic Thrustbelts and Basins of Central and Eastern Europe. EAGE Special Publication, pp. 331-341.

Steckler, M. S. and Watts, A. B. (1978). Subsidence of the Atlantic-type continental margin off New York. Earth and Planetary Science Letters, 41, 1-13.

Steininger, F. F. and Wessely, G. (1999). From the Tethyan Ocean to the Paratethys Sea: Oligocene to Neogene Stratigraphy, Paleogeography and Palaeobiogeography of the circum-Mediterranean region and the Oligocene to Neogene Basin evolution in Austria. Mitteilungen der Österreichischen Geologischen Gesellschaft, 92, 95-116.

Strauss, P., Harzhauser, M., Hinsch, R. and Wagreich, M. (2006). Sequence stratigraphy in a classic pull-apart basin (Neogene, Vienna Basin) - A 3D seismic based integrated approach. Geologica Carpathica, 57, 185-197.

Van Hinte, J. E. (1978). Geohistory analysis - Application of micropaleontology in exploration geology. AAPG Bulletin, 62, 201-222.

Wagreich, M. (1991). Subsidenzanalyse an kalkalpinen Oberkreideserien der Gosau-Gruppe (Österreich). Zentralblatt für Geologie und Paläontologie, Teil 1, 1990, 1645-1657.

Wagreich, M. and Schmid, H.-P. (2002). Backstripping dip-slip fault histories: apparent slip rates for the Miocene of the Vienna Basin. Terra Nova, 14, 163-168.

Weissenbäck, M. (1996). Lower to Middle Miocene sedimentation model of the central Vienna Basin. In: Wessely, G. and Liebl, W. (eds.), Oil and Gas in Alpidic Thrustbelts and Basins of Central and Eastern Europe. EAGE Special Publication, pp. 355-363.

Wessely, G. (1988). Structure and Development of the Vienna Basin in Austria. In: Royden, L. and Horvath, F. (eds.), The Pannonian Basin-A Study in basin evolution. AAPG Memoir, pp. 333-346.

Wessely, G. (1992). The Calcareous Alps below the Vienna Basin in Austria and their structural and facial development in the Alpine-Carpathian border zone. Geologica Carpathica, 43, 347-353.

Monika HÖLZEL[1)*)], Michael WAGREICH[1)], Robert FABER[2)] & Philipp STRAUSS[3)]

[1)] Department of Geodynamics and Sedimentology, University of Vienna, Centre for Earth Sciences, Althanstr. 14, 1090 Vienna, Austria

[2)] Terramath, Hauptstr. 59, 3021 Pressbaum, Austria

[3)] OMV Exploration & Production GmbH, Gerasdorferstr. 151, 1210 Vienna, Austria

[*)] Corresponding author, monika.hoelzel@univie.ac.at